



ELSEVIER

Contents lists available at ScienceDirect

Chemical Geology

journal homepage: [www.elsevier.com/locate/chemgeo](http://www.elsevier.com/locate/chemgeo)

Cycles of trace elements and isotopes in the ocean – GEOTRACES and beyond

## Barite formation in the ocean: Origin of amorphous and crystalline precipitates<sup>☆</sup>

F. Martinez-Ruiz<sup>a,\*</sup>, A. Paytan<sup>b</sup>, M.T. Gonzalez-Muñoz<sup>c</sup>, F. Jroundi<sup>c</sup>, M.M. Abad<sup>d</sup>, P.J. Lam<sup>b</sup>, J.K.B. Bishop<sup>e</sup>, T.J. Horner<sup>f</sup>, P.L. Morton<sup>g</sup>, M. Kastner<sup>h</sup>

<sup>a</sup> Instituto Andaluz de Ciencias de la Tierra (CSIC-UGR), Avda. de las Palmeras 4, 18100 Armilla, Granada, Spain

<sup>b</sup> Institute of Marine Sciences, University of California Santa Cruz, Santa Cruz, CA 95064, USA

<sup>c</sup> Department of Microbiology, Faculty of Science, University of Granada, Campus Fuentenueva, Granada 18002, Spain

<sup>d</sup> Centro de Instrumentación Científica (CIC), University of Granada, Campus Fuentenueva, Granada 18071, Spain

<sup>e</sup> Department of Earth and Planetary Science, UC Berkeley, Berkeley, CA, 94720, USA

<sup>f</sup> Department of Marine Chemistry and Geochemistry, Woods Hole Oceanographic Institution, Woods Hole, MA 02543-1050, USA

<sup>g</sup> National High Magnetic Field Lab. Florida State University, Tallahassee, FL 32310, USA

<sup>h</sup> Scripps Institution of Oceanography, University of CA San Diego, La Jolla, CA 92037, USA

### ARTICLE INFO

Editor: Michael E.B.

#### Keywords:

Marine barite  
Ocean productivity  
Bacteria  
Biofilms  
EPS  
Barite precipitation

### ABSTRACT

Ocean export production is a key constituent in the global carbon cycle impacting climate. Past ocean export production is commonly estimated by means of barite and Barium proxies. However, the precise mechanisms underlying barite precipitation in the undersaturated marine water column are not fully understood. Here we present a detailed mineralogical and crystallographic analysis of barite from size-fractionated particulate material collected using multiple unit large volume in-situ filtration systems in the North Atlantic and the Southern Ocean. Our data suggest that marine barite forms from an initial amorphous phosphorus-rich phase that binds Ba, which evolves into barite crystals whereby phosphate groups are substituted by sulfate. Scanning electron microscopy observations also show the association of barite particles with organic matter aggregates and with extracellular polymeric substances (EPS). These results are consistent with experimental work showing that in bacterial biofilms Ba binds to phosphate groups in both cells and EPS, which promotes locally high concentrations of Ba leading to saturated microenvironments favoring barite precipitation. These results strongly suggest a similar precipitation mechanism in the ocean, which is consistent with the close link between bacterial production and abundance of Ba-rich particulates in the water column. We argue that EPS play a major role in mediating barite formation in the undersaturated oceanic water column; specifically, increased productivity and organic matter degradation in the mesopelagic zone would entail more extensive EPS production, thereby promoting Ba bioaccumulation and appropriate microenvironments for barite precipitation. This observation contributes toward better understanding of Ba proxies and their utility for reconstructing past ocean export productivity.

This article is part of a special issue entitled: “Cycles of trace elements and isotopes in the ocean – GEOTRACES and beyond” - edited by Tim M. Conway, Tristan Horner, Yves Plancherel, and Aridane G. González.

### 1. Introduction

The biogeochemistry of barium has intrigued geochemists for decades because of its nutrient-like distribution in seawater and its precipitation as barite in the water column despite widespread undersaturation conditions (Monnin et al., 1999). To explain this apparent

contradiction, it has been suggested that barite precipitates in barite-supersaturated microenvironments generated by the biological degradation of sinking organic matter. Since the early sixties (e.g., Chow and Goldberg, 1960) a vast literature on Ba has provided evidence for a link between barite formation in the ocean and biological activity. Dehairs et al. (1980) and Bishop (1988) proposed that decomposition of

<sup>☆</sup> This article is part of a special issue entitled: “Cycles of trace elements and isotopes in the ocean – GEOTRACES and beyond” - edited by Tim M. Conway, Tristan Horner, Yves Plancherel, and Aridane G. González.

\* Corresponding author.

E-mail address: [fmruiz@ugr.es](mailto:fmruiz@ugr.es) (F. Martinez-Ruiz).

<https://doi.org/10.1016/j.chemgeo.2018.09.011>

Received 12 June 2018; Received in revised form 10 August 2018; Accepted 9 September 2018

Available online 06 October 2018

0009-2541/ © 2018 The Authors. Published by Elsevier B.V. This is an open access article under the CC BY-NC-ND license

(<http://creativecommons.org/licenses/by-nc-nd/4.0/>).



Fig. 1. Location map showing the two sampled sites at the North Atlantic and the Southern Ocean.

**Table 1**  
Analyzed samples at the North Atlantic and the Southern Ocean sites.

Samples	Depth (m)	Location
North Atlantic		39 28.620 N 64 50.820 E
R 412	193	
R 404	227	
R 430	326	
Southern Ocean		50 23.993 S 10 48.009 W
GCM 93	25	
GCM 94	59	
GCM 95	109	
GCM 96	159	
GCM 97	300	
GCM 98	500	
GCM 99	750	
GCM 100	1000	
GCM 101	1020	

organic matter debris might provide the appropriate microenvironment for barite precipitation. Subsequent studies in the Southern ocean (Dehairs et al., 1991; Stroobants et al., 1991) also demonstrated barite precipitation in saturated microenvironments within bio-aggregates. Nevertheless, despite decades of research, the precise mechanism for the precipitation of Ba as barite in undersaturated conditions is still unknown. Although a clear association to organic matter production and carbon fluxes to depth has been widely demonstrated (e.g., Dehairs et al., 1980; Dymond et al., 1992; Paytan et al., 1996; Griffith and

Paytan, 2012), and broadly supported by Ba isotopes studies (Horner et al., 2015; Cao et al., 2016; Bates et al., 2017; Bridgestock et al., 2018), the exact mechanisms for nucleation and crystallization are not fully understood. This is of major importance since barium fluxes to the deep ocean and barite accumulation in sediments have been widely used as a proxy to reconstruct past ocean export productivity (Paytan et al., 1996; Paytan and Griffith, 2007), which in turn has implications for reconstructions of the marine carbon cycle and global climate.

A possible link between barite formation and microbial activity has also been suggested based on the correlation between the abundance of bacteria and barite in the ocean water column. Specifically, it has been shown that higher mesopelagic particulate Ba correlates with greater bacterial production, suggesting a potential relationship (Dehairs et al., 2008; Jacquet et al., 2011; Planchon et al., 2013). The capability of certain marine bacteria to mediate barite precipitation under experimental conditions has also been demonstrated, which suggested that bacteria play a role in mediating barite precipitation in natural environments (González-Muñoz et al., 2003, 2012; Torres-Crespo et al., 2015). However, the specific association between Ba and organic matter in such microenvironments remain poorly understood. Ganeshram et al. (2003) also demonstrated using mesocosm phytoplankton decay experiments that barite crystals precipitate within particle-associated microenvironments supplied with additional barium ions derived from heterotrophic remineralization of organic matter. Most recently, Horner et al. (2017) presented evidence of pelagic barite formation at extreme barite undersaturation (in Lake Superior), further supporting the notion that barite precipitation occurs in protected microenvironments.

Traditionally most of the laboratory research on biogenic or biologically mediated mineral precipitation has focused on carbonates and iron minerals, and not microbial precipitation of sulfates. An initial experimental approach to explore bacterial barite precipitation served to demonstrate that a soil bacterium, with a well-known biomineralization capability in culture experiments (*Myxococcus xanthus*), could mediate the precipitation of barite (González-Muñoz et al., 2003). Tazaki et al. (1997), Glamoclija et al. (2004), Sanchez-Moral et al. (2004) and Senko et al. (2004) also reported barite precipitation in natural settings in which bacteria have played a role either in oxidizing sulfur compounds to generate sulfate or in providing biofilms in which precipitation occurs. Similarly, in a warm sulfur spring in Canada, Bonny and Jones (2008) reported barite crystals that nucleated on microbial cell surfaces and in microbial EPS. Follow-up experiments with marine bacteria demonstrated that several marine strains have the capability to precipitate barite under laboratory conditions (González-Muñoz et al., 2012). Stevens et al. (2015) have demonstrated the precipitation of barite on filaments of sulfide-oxidizing bacteria in marine cold seep, and Widanagamage et al. (2015) have also shown the precipitation of barite in microbial biomass in modern continental environments. Nonetheless, the experimental cultures as well as settings in which the bacterial metabolism is responsible for providing the necessary sulfur for barite precipitation (as in the above studies) are not analogous to the ocean environment where sulfate is abundant and present in excess relative to Ba.

In general, there are two means to precipitate barite in natural settings: adding sulfate to a Ba-rich fluid, or by adding Ba to a sulfate-rich fluid (e.g., Hanor, 2000). Since seawater contains abundant sulfate compared to barium, the latter scenario is significantly more likely to control barite precipitation in the ocean. Indeed, emerging results from laboratory (e.g., Martínez-Ruiz et al., 2018) and the aforementioned field studies suggest that bacteria—and in particular, bacterial biofilms—appear to play an important role in creating local elevations in Ba concentration that can subsequently interact with (ambient) sulfate

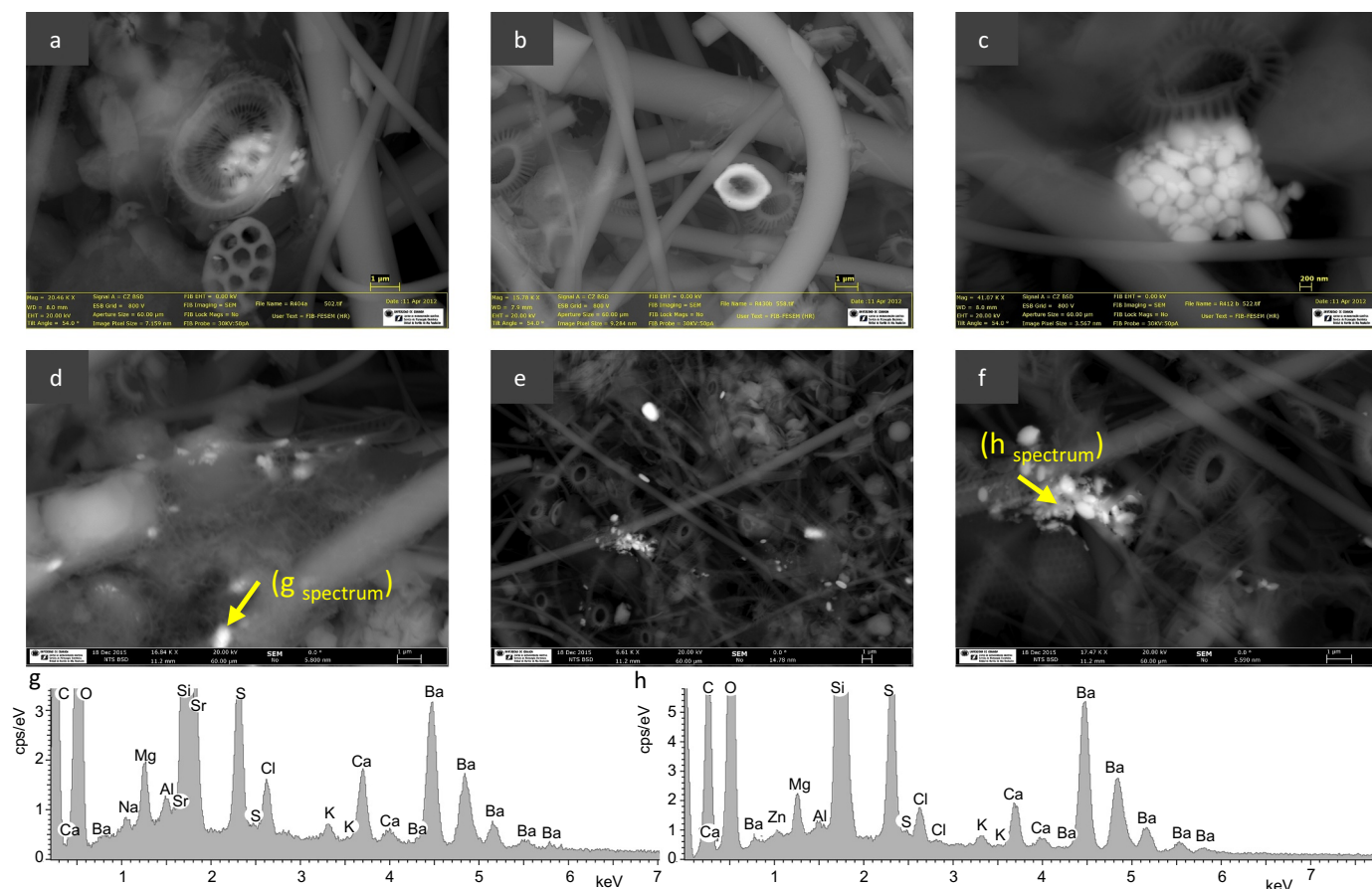


**Fig. 2.** SEM photographs showing representative examples of barite particles from the North Atlantic sector obtained in backscattered electron (BSE) mode at 30 kV: a, sample R404 (227 m depth); b, sample R430 (326 m depth); c-d-e-f, sample R 412 (193 m depth); g and h, correspond to the SEM-EDX spectra obtained from the spot marked with an arrow in BSE images d and f respectively. The vertical scale is enlarged to show the relative intensities of S and Ba peaks since large Si peaks are obtained due to the quartz filter substrate. Ba is consistently identified by lines Ba-LA, LB1, LB3, LB2 and LG1 (from left to right) in EDX spectra.

to promote barite nucleation. However, the exact mechanism(s) by which barium is concentrated during pelagic barite precipitation remain to be identified.

Here we present new mineralogical and crystallographic data from natural barite particles from the oceanic water column (upper 1000 m) in order to shed light on mechanisms for barite nucleation and crystallization, and to constrain the link between bacterial activity, Ba bioaccumulation, and barite precipitation in the ocean water column.

## 2. Material and methods

Size-fractionated particulate material was collected using multiple unit large volume in-situ filtration system (MULVFS; Bishop et al., 1985) and battery-operated McLane in-situ pumps (LV-WTS) (Rosengard et al., 2015). Samples were collected during two expeditions: one in the North Atlantic, during R/V Knorr cruise 98 (WCR 82H in September 1982), and in the Southern Ocean (Atlantic Sector), at Station 92 of MV1101 (February 2011; Balch et al., 2016) (Fig. 1, Table 1). From both expeditions, quartz fiber filters (Whatman QMA) representing the 1–51  $\mu\text{m}$  size fraction (from the upper 326 and 1020 m respectively) were examined under scanning electron microscopy (SEM) and high-resolution transmission electron microscopy (HRTEM). Particulate Ba concentrations were also determined on the 1–51  $\mu\text{m}$  size

fraction but on acid-cleaned PES (polyethersulfone) membrane filters (Pall Gelman ‘Supor’), deployed at the same time as the quartz-fiber filters (see Bishop et al., 2012). Sample depths and locations are provided in Table 1.

Selected filter pieces were coated with carbon for observation under the SEM using an AURIGA FIB- FESEM Carl Zeiss SMT microscope equipped with an energy dispersive X-ray (EDX) detector system (Centre for Scientific Instrumentation, University of Granada). For HRTEM, filter pieces were grounded in an agate mortar and then dispersed in ethanol by sonication for approximately 3 min. Particulate matter from the samples were then collected and deposited on carbon-film-coated copper grids for the observation in a FEI TITAN G2 60–300 microscope with a high brightness electron gun (X-FEG) operated at 300 kV and equipped with a Cs image corrector CEOS (Centre for Scientific Instrumentation, University of Granada). For analytical electron microscopy (AEM), a SUPER-X silicon-drift windowless EDX detector was also used. Digital X-ray maps and selected area electron diffraction (SAED) patterns were collected on barite particles.

Dissolved and particulate Ba distributions were determined in the upper 1000 m of the water column at St. 92 (Southern Ocean). In situ-deployed filters were processed using the protocol described in Bishop and Wood (2008), whereby subsamples of the PES membrane were leached in 0.6 M HCl overnight (~16 h) at 60 °C in acid-cleaned PTFE

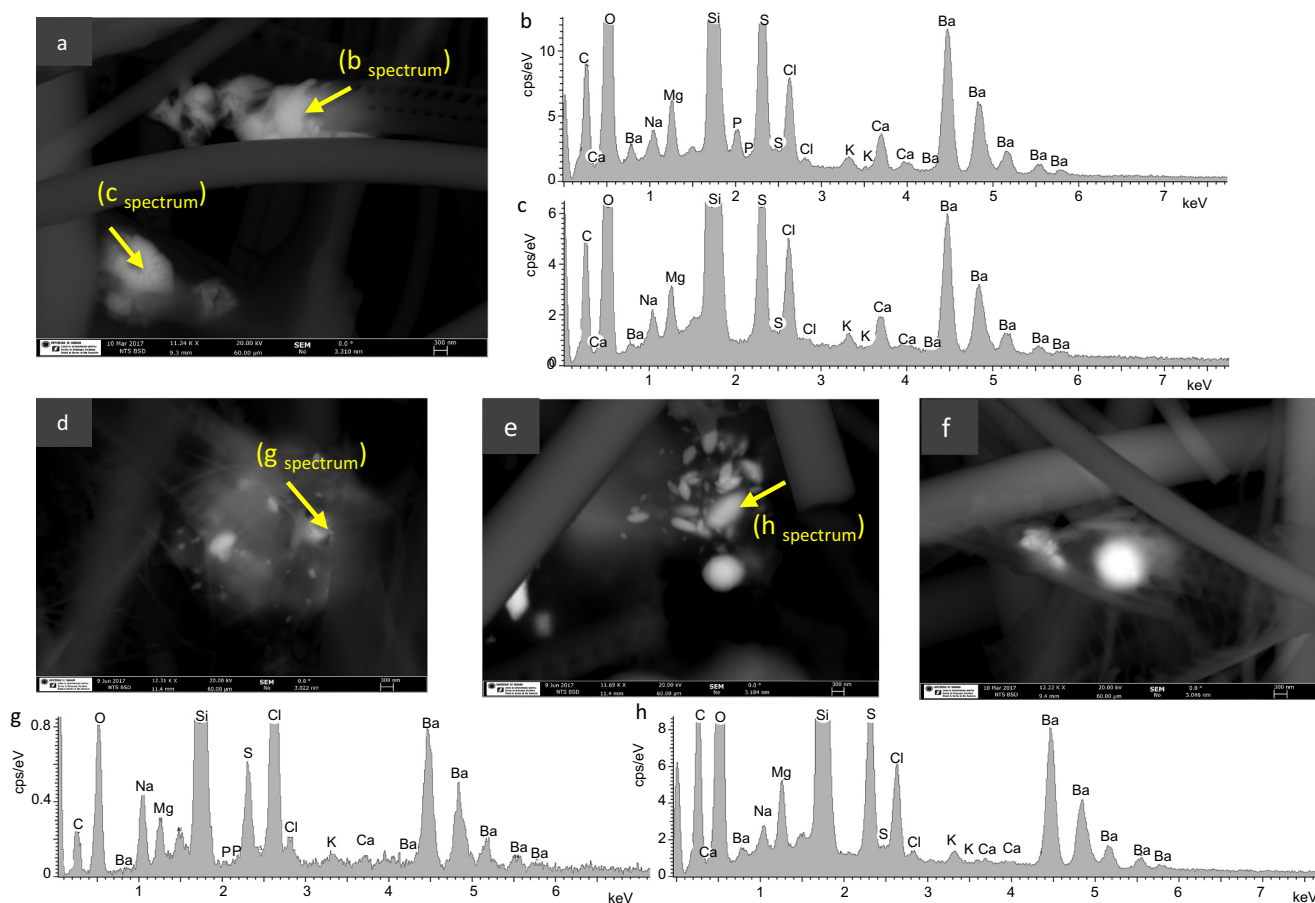


Fig. 3. SEM photographs showing representative examples of barite particles from the Southern Ocean (sample GCM 100, 1000 m depth) obtained in backscattered electron (BSE) mode at 30 kV: a–c, photograph and two selected SEM-EDX spectra (analyzed spot marked with an arrow in BSE image). As indicated in Fig. 2, the vertical scale is enlarged to show the relative intensities of S and Ba peaks since large Si peaks are obtained due to the quartz filter substrate. The variable P content in barite particles is shown in the respective spectra; d–f show other examples of barite occurrence and composition of selected particles (indicated in d and e) is given in the corresponding spectra (g and h).

vials. Concentrations of Ba and phosphorus were determined using a ThermoFinnigan ELEMENT II ICP-MS as per Horner et al. (2017), with quantification achieved via comparison of blank- and indium-normalized sample ion beam intensities to those of reference standards of known Ba and P concentrations. Seawater samples were collected using nine 5-L Niskin-X bottles (General Oceanics) suspended at nine depths from Kevlar line. Samples were filtered using acid-washed Acropak-200 filter capsules, collected into acid-washed 250-mL wide mouth Nalgene HDPE bottles, and acidified to 0.024 M HCl (pH 1.7) using concentrated HCl (Fisher Optima). Dissolved Ba concentrations were determined by diluting aliquots of the acidified seawater samples by a factor of 25 into 0.32 M HNO<sub>3</sub> (double distilled; Savillex Teflon still) and analyzed by direct injection into an ELEMENT 2 HR-ICP-MS (medium resolution). Concentrations were quantified by external standards (High Purity Standards, South Carolina) after normalizing by the measured Sr-88 signal (medium resolution) and assuming a constant seawater Sr concentration of 92.8 nM. Seawater Sr was used as the internal standard, rather than Ba isotope dilution, since samples needed to be preserved for subsequent Ba stable isotope ratio determinations. Barium blanks were determined to be less than 0.05 nM (or less than 2% of the measured Ba concentrations), and dissolved Ba concentrations in triplicate measurements of consensus reference materials GEOTRACES GSP and

SAFe D1 were determined to be  $35.2 \pm 0.54$  nM and  $96.3 \pm 0.52$  nM, respectively.

### 3. Results

Barite particles were observed in all analyzed filters. The observed crystal morphologies are rounded or elliptical and sizes usually range from 200 nm to 2 μm. These morphologies are similar to those reported in previous studies of barite from the water column and to ellipsoidal barite grains from marine sediments (Dehairs et al., 1980; Stroobants et al., 1991; Bertram and Cowen, 1997; Gingele and Dahmke, 1994; Griffith and Paytan, 2012). Figs. 2 and 3 show water column barite particles from the two studied regions, the North Atlantic and the Southern Ocean. Barite is mostly observed in microenvironments rich in biogenic debris often forming aggregates within these microenvironments, which associate with EPS like material (Figs. 3 and 4). EDX analyses provide the composition of these barite grains and show that in some cases the grains contain appreciable amounts of P. The aggregates in which the barite is seen have also been analyzed and they also contain P. In general, bigger grains that correspond to more evolved stages are composed of purer Ba-sulfate, while smaller grains, that likely correspond to initial stages of formation, are richer in P (Fig. 3).

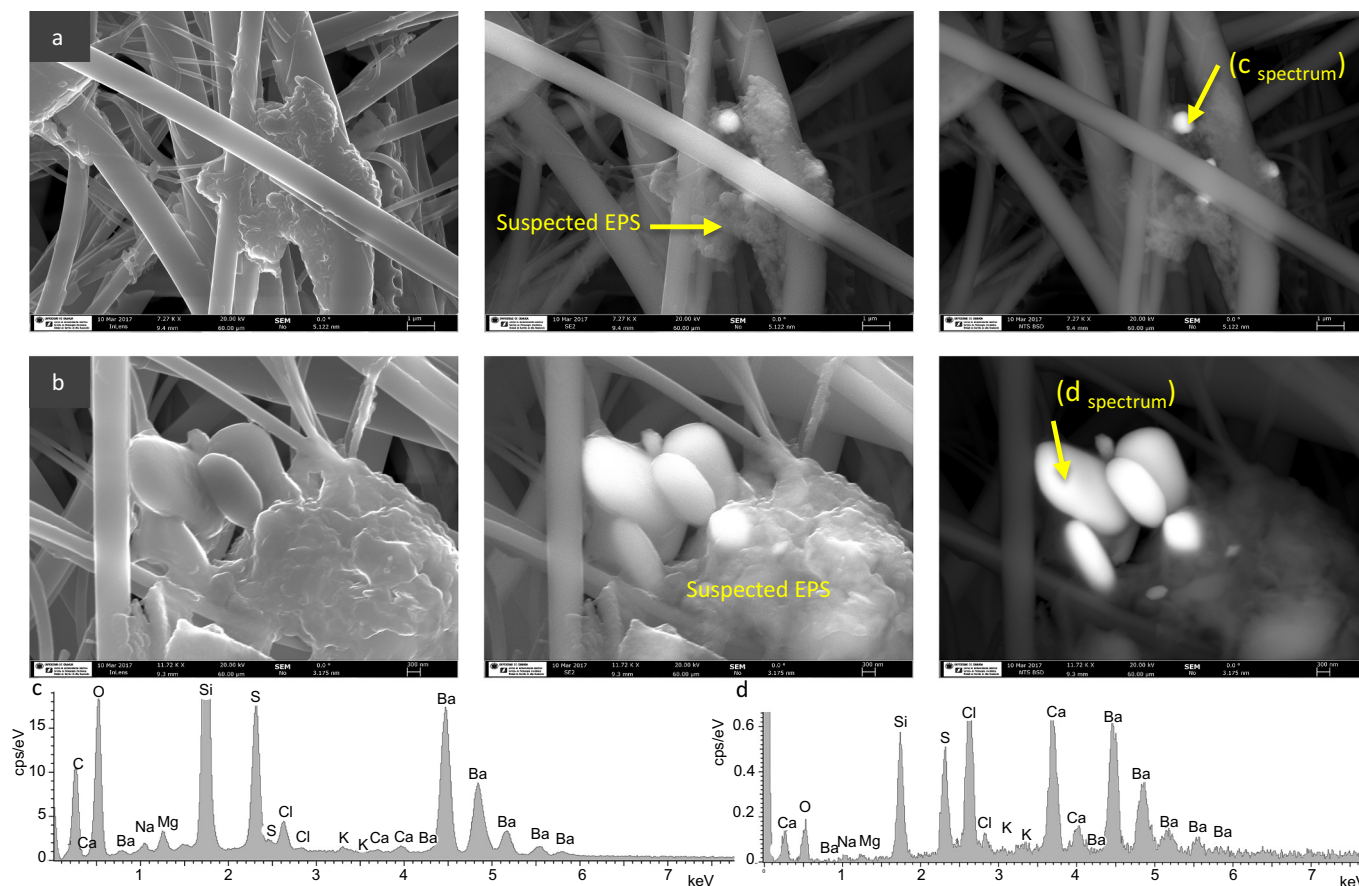


**Fig. 4.** Representative examples of barite grains, linked to suspected EPS observed among the quartz fibers of the filter, from Southern Ocean samples GCM 100, 1000 m depth (a, upper images) and GCM 99, 750 m depth (b, lower images). Photographs were obtained under three different SEM observation modes: Inlens detector (left), secondary (central) and backscattered electron mode (right). c and d, correspond to selected SEM-EDX spectra (analyzed spot marked with an arrow in BSE images a and b respectively). The vertical scale is enlarged to show the relative intensities of S and Ba peaks since large Si peaks are obtained due to the quartz filter substrate.

Certain grains Sr is also detected (Fig. 2). The exact composition has been determined by HRTEM. A whole range of compositions from P-rich grains to barite crystals has been recognized (Figs. 5 and 6). EDX maps and spectra also show that the distribution of Ba, P, and S in the precipitates is not homogeneous with domains richer in P (Fig. 5). Ba-phosphate particles have been observed in which S rich domains are also observed (Fig. 6). A wide range of degrees of crystallinity has also been recognized. The P-rich precipitates are mostly amorphous or very poorly crystallized (Fig. 7), as evidenced by HRTEM and SAED images. In contrast, barite precipitates are crystalline and SAED images evidence the d-spaces of barite crystals. These barite crystals also show a more homogeneous composition (Fig. 8) with lower P content and a regular distribution of S and Ba.

The samples from North Atlantic sector were also analyzed by SEM at UC Berkeley shortly after collection in 1982, and these images show what seems to be coccus bacteria associated with barite (Fig. 9).

Dissolved and particulate data from the Southern Ocean (Fig. 10) show features consistent with those of published from other regions. Specifically, the particulate data show a maximum in particulate P of  $\approx 34$  nM at the base of the  $E_z$  (euphotic zone, 59 m at St. 92; Rosengard et al., 2015), which sharply decreases to values  $\approx 1$  nM throughout much of the mesopelagic. Conversely, pBa is generally low ( $\approx 318$  pM) at the base of the  $E_z$ , increasing to a maximum of  $\approx 519$  pM near the top

of the mesopelagic, before decreasing gently to values  $\approx 277$  pM by 1000 m. Despite the increasing-then-decreasing nature of the pBa profile (Fig. 10), the resultant pBa:pP of bulk particulate matter monotonically increases throughout the profile.

#### 4. Discussion

The nature and characteristics of barite particles from the ocean water column can shed light into the mechanisms leading to saturation and precipitation of barite in microenvironments within sinking particulate matter. We detect a range of particle sizes, compositions and crystallinity ranging from amorphous, small Ba-P associations to slightly larger crystalline barite particles. Strontium was also observed in some of the particles.

Stroobants et al. (1991) showed that in the first 10–20 m of the water column in the Southern Ocean barite particles appear in bioaggregates as amorphous entities without a clear crystalline habit while at greater depths the particles have typical crystalline habits which likely reflects progression toward pure barite crystals. The morphology of suspended barite and that from sediments has also been studied in previous works (e.g., Dehairs et al., 1980; Stroobants et al., 1991; Bertram and Cowen, 1997; Gingele and Dahmke, 1994; Griffith and Paytan, 2012) and differences have been reported. While suspended

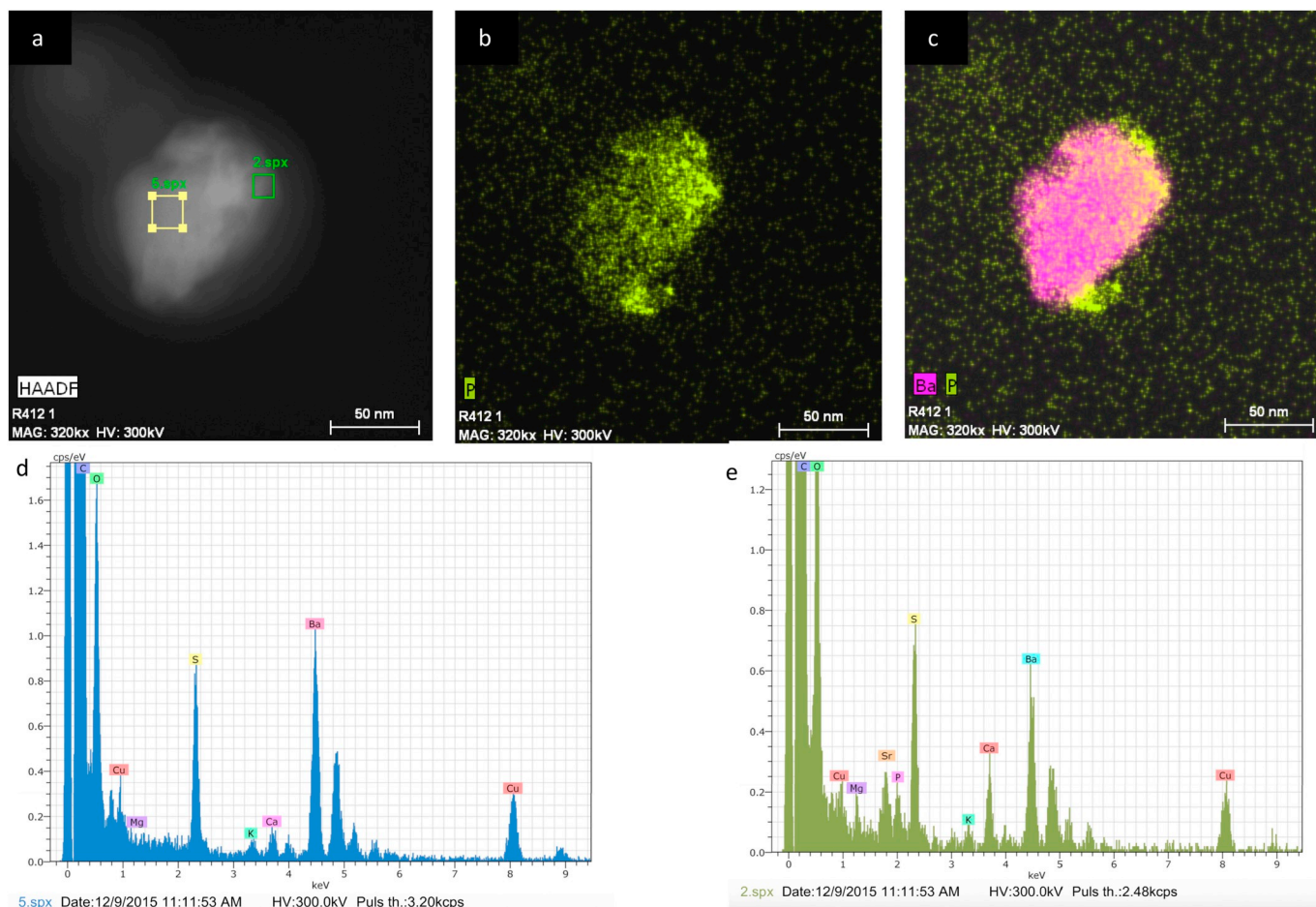


**Fig. 5.** High Angle Annular Dark Field (HAADF) STEM image (a) and corresponding EDX maps showing the distribution of P (b) and Ba plus P (c) in a barite particle from sample R 412 (193 m depth, North Atlantic) and representative spectra indicated in the HAADF image, 5.xps (d) and 2.xps (e). Note the difference in P and Sr content within the same nanosize particle. Sr is clearly identified since the Si from the quartz filter substrate is not overlapping the Sr peak as occurring in SEM EDX spectra.

barite is observed mostly as sub-micron ellipsoidal crystals, barite crystals found in sediments are generally bigger and mostly euhedral, having well defined crystal habits. Differences in morphology have also been related to Sr content in barite precipitates. [Bertram and Cowen \(1997\)](#) suggested a correlation with crystal shape since elongated hexagonal crystals do not usually contain detectable Sr while ellipsoidal crystals contain more Sr. Part of the Sr may be lost with exposure to undersaturated seawater due to the higher solubility of Sr rich barite ([Rushdi et al., 2000](#); [van Beek et al., 2003](#)). Similar trends in Sr incorporation into barite have also been previously reported by [Bishop \(1988\)](#). Collectively, this variability represents various stages in the process of barite formation in the water column and the transformation to the crystals found in marine sediments.

#### 4.1. Microbial mediation

In some natural settings microbes have been shown to mediating barite formation, either via oxidizing sulfur compounds (to generate sulfate) or providing biofilms for bioaccumulation of Ba (promoting barite nucleation; e.g., [Tazaki et al., 1997](#); [Glamoclija et al., 2004](#), [Sanchez-Moral et al., 2004](#), [Senko et al., 2004](#); [Bonny and Jones, 2008](#); [Stevens et al., 2015](#); [Widanagamage et al., 2015](#); [Singer et al., 2016](#)). Moreover, laboratory experiments performed with isolates of sulfide-

oxidizing bacteria demonstrated that under low sulfate conditions, the sulfate generated by the sulfide-oxidizing bacteria fosters rapid barite precipitation localized to the cell biomass. Similarly, in experiments where sulfate was not present in the culture medium (to avoid inorganic precipitation; [González-Muñoz et al., 2003, 2012](#)), bacterial metabolism was responsible for sulfate production. This study strongly suggests that bacterial biofilms and EPS production in the ocean could account for barite formation in marine microenvironments. The bacterial biomass would contribute to concentrating barium thus providing the necessary binding sites for barite formation. In fact, the capability of bacterial biomass to accumulate metals has been broadly demonstrated (e.g., [Kuyucak and Volesky, 1988](#); [Kikuchi and Tanaka, 2012](#)). Bacteria have the capability to immobilize diverse metals such as U (e.g., [Merroun and Selenska-Pobell, 2008](#)), and it has also been demonstrated that some marine bacteria (*Idiomarina* sp. PR58-8) are highly metal-tolerant, for instance are able to synthesize silver nanoparticles (e. g., [Sheshadri et al., 2012](#)). In the case of Ba, it was also demonstrated that a soil bacterium, *M. xanthus*, has the capability to bioadsorb Ba on both the cell membranes and on the EPS produced by this bacterium ([Merroun, 1999](#)).

Our results from the above observations of natural barite precipitates collected in the water column further support this hypothesis, particularly our observations of barite forming: within EPS ([Fig. 4](#)), in

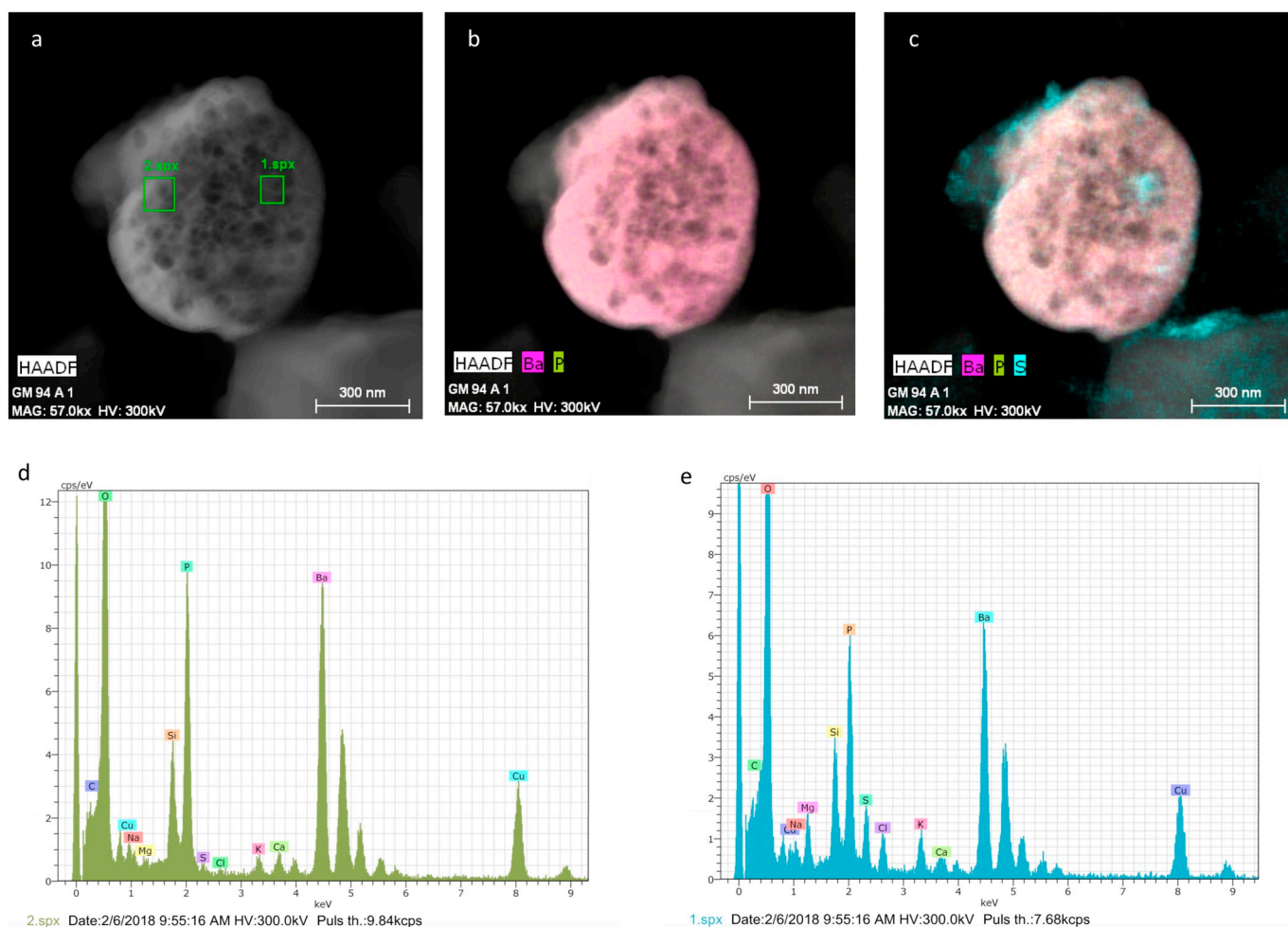


**Fig. 6.** High Angle Annular Dark Field (HAADF) STEM image (a) and corresponding EDX maps showing the distribution of Ba and P (b), and Ba, S and P (c) in a particle with Ba phosphate composition (Southern Ocean sample GCM 94, 59 m depth). The spectra indicated in the HAADF image (a) also show the significant P enrichment: 2.spx (d) and 1.spx (e).

close association with organic matter aggregates (Figs. 2 and 3), and in presence of barite-mineralized coccus bacteria (Fig. 9), as direct evidence in support of this mechanism. Evidence of barite abundance linked to enhanced bacterial activity in the ocean further reinforces this hypothesis. Dehairs et al. (2008) investigated particulate Ba content in the North Pacific and demonstrated that the vertical distribution of particulate non-lithogenic Ba in the water column is positively correlated with bacterial production. In the Australian sector of the Southern Ocean Jacquet et al. (2011) also observed that increasing content of mesopelagic particulate Ba was correlated with higher bacterial activity. Similarly, Planchon et al. (2013) have also shown that mesopelagic particulate Ba distribution reflects bacterial degradation of organic matter and is related to oxygen consumption and bacterial carbon respiration in the Atlantic sector of the Southern Ocean.

The relation between Ba and biological processes in the water column is also manifested in the distribution of particulate and dissolved Ba in the water column (Fig. 10). At station 92 the sub-surface maxima in particulate Ba illustrates the uptake of Ba from the dissolved phase into particulate barite. The particulate P at this station—a proxy for total particulate organic matter—is also highest near the surface and decreases with depth throughout the water column along a power-law

trajectory (e.g., Martin et al., 1987; Rosengard et al., 2015). This pattern reflects an intense remineralization of organic matter in the upper water column. The reduction in particulate P is often found to occur around the same depths at which particulate Ba increases; indeed, the sharpest drop in particulate P is coincident with the sharpest increase in particulate Ba (between 59 → 109 m). This is also consistent with the nutrient-like profile observed for dissolved [Ba], whereby most dissolved Ba removal occurs below the euphotic zone, but before the supply of particulate organic matter has completely attenuated (top few hundred meters). Thus the resultant dissolved profile is similar to most other nutrients in that [Ba] exhibits the lowest concentration at or near the surface. Similar trends in dissolved and particulate Ba are observed throughout the ocean water column and have been used to support the link between organic matter oxidation and barite abundance at mesopelagic depths (e.g., Dehairs et al., 1997; Jacquet et al., 2004; Horner et al., 2015; Pyle et al., 2018).

Based on our observations and previous data we conclude that barite precipitation in the ocean water column is mediated by Ba enrichment by bacterial activity in microenvironments of sinking organic aggregates where bacteria abundantly produce exopolymers.

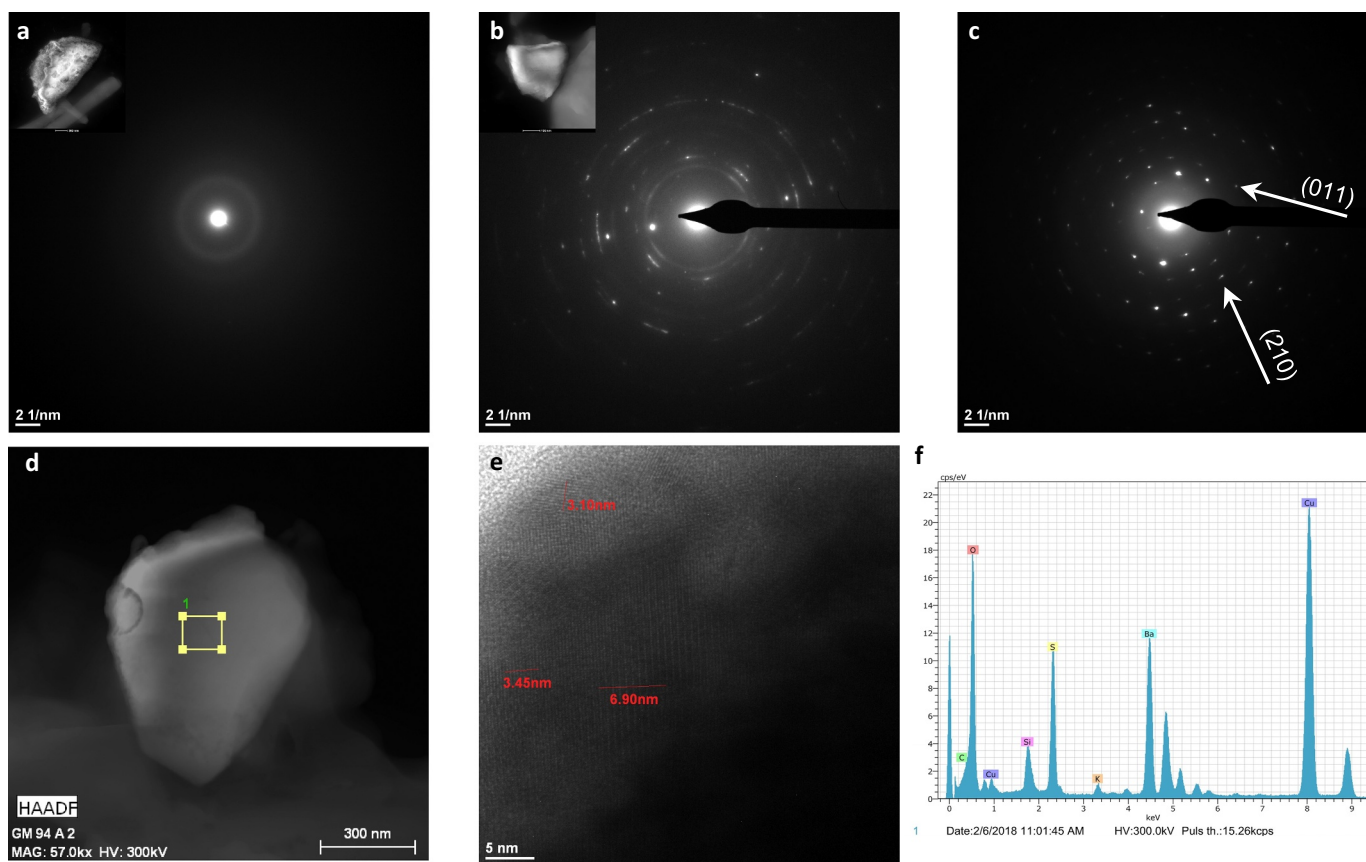


Fig. 7. Selected area electron diffraction (SAED) images obtained by HRTEM showing the diverse degree of crystallinity in barite particles: a shows amorphous precipitates, while b and c show well-crystallized barite, the characteristic d-spaces of are clearly observed: 3.45 Å (210) and 4.34 Å (011) (c). d corresponds to a High Angle Annular Dark Field (HAADF) STEM image (sample GCM 94, 59 m depth) and e shows a lattice-fringe image where d-spaces characteristic of barite are indicated: 3.45 Å (210) and 3.10 Å (211). In both cases as ten unit cells have been measured, the d-spaces in Å correspond to the indicated nm values. The corresponding spectrum (f) indicated in image in the STEM image (d) shows the barite composition.

#### 4.2. Amorphous and crystalline precipitates

Experimental work has shown that Ba enrichment in bacterial cells and EPS occurs by binding to phosphate groups in the bacterial biomass (González-Muñoz et al., 2012; Martínez-Ruiz et al., 2018). Indeed, the binding to phosphate is a common process in microbial mineral precipitation. This mechanism has been shown for Ba bioabsorption by soil bacteria (Merroun, 1999) and has also been demonstrated in barite precipitation in culture experiments (González-Muñoz et al., 2003, 2012; Torres-Crespo et al., 2015). In general, the ability of polyphosphates to chelate metal ions has been broadly verified. It has been proposed that the intracellular chelation of heavy metals by polyphosphate can serve to decrease heavy metal toxicity, which improves cellular tolerance to metals (Keasling and Hupf, 1996; Merroun and Selenska-Pobell, 2008). Phospholipids likely act as nucleation sites to incorporate Ba, as has also been shown for other metals such as U (Morcillo et al., 2014). Importantly, a P-rich precursor has been described in the microbial precipitation of other minerals in culture experiments, for instance the nucleation of an amorphous phosphate phase has been recognized in microbial aragonite precipitation (Rivadeneira et al., 2010) and also reported for bacterial biomineralization of apatite and iron oxides both in laboratory experiments and in the geological record (e.g. Sanchez-Navas and Martin-Algarra, 2001;

Miot et al., 2009). Though phosphate and sulfate groups have different ionic radii, with the phosphate group being larger, the substitution of sulfate and phosphate groups for one other is a common process in nature as are solid solutions between phosphate and sulfate minerals (e.g., Rinaudo et al., 1994; Secco et al., 2015). Interestingly, the formation of Ba phosphate phases has been described in bio-cements formed by microbially-induced mineralization in experimental conditions. In loose sand particles, such minerals play a role in the binding between loose sand particles and the bio-cement (Qian et al., 2018). Our observations from natural barite demonstrate that the phosphate groups are the precursor ligand for Ba that is eventually substituted by sulfate. Both the composition and the crystallinity of natural barites support this mechanism for precipitation through an amorphous P-rich precursor. As revealed by HRTEM a Ba-phosphate link is initially formed that eventually evolves to barite. This P-rich phase is mostly amorphous at the initial stages of crystallization and is suggested to be the phase binding Ba though the strong attractive interactions of Ba and sulfate lead to a more stable mineral phase as barite. Barite crystals are clearly identified by distinctive d-spaces (Figs. 7 and 8).

#### 4.3. Role of exopolymers in barite precipitation

In high productivity regions, where high organic matter degradation



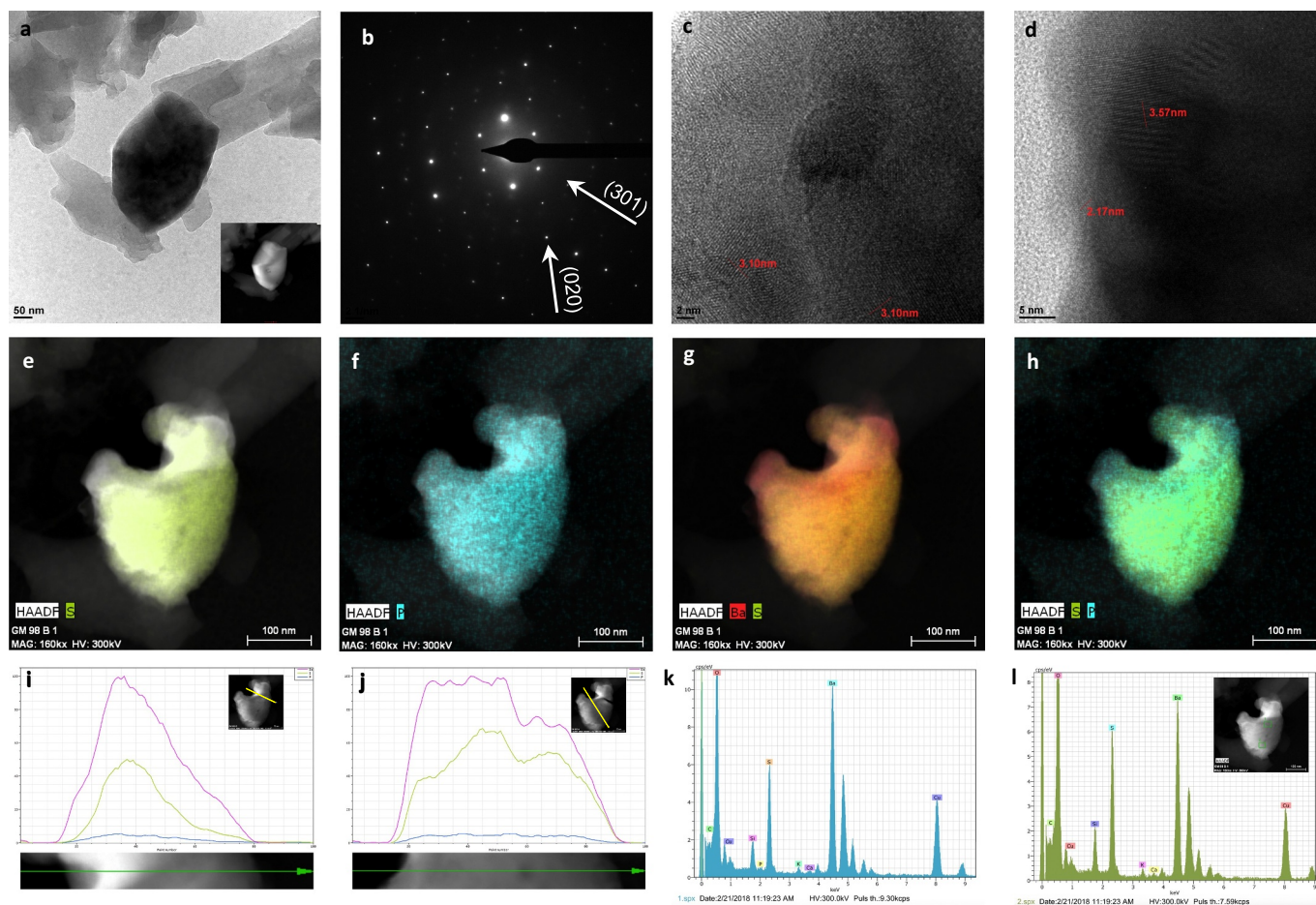


**Fig. 8.** High Angle Annular Dark Field (HAADF) STEM image (a), and selected area electron diffraction (SAED) image (b) showing the crystallinity of a representative barite particle from sample GCM 94, 59 m depth. Lattice-fringe images (c and d) show d-spaces characteristic of barite: 3.10 Å (211), 2.17 Å (022), and 3.57 Å (002); as ten unit cells have been measured, the d-spaces in Å correspond to the indicated nm values. EDX maps (e–h) show the distribution of Ba, S, and P, and profiles (i–j) show element abundance across the particle, also evidenced by EDX spectra (k–l), the analyzed areas are indicated in the image included in the right spectrum (l): 1.xps (k) and 2.xps (l).

involves higher bacterial activity, extensive EPS production would also be expected. Such a link would also be consistent with the observed relationship between export productivity, bacterial activity, and barite formation in the ocean. Our observations strongly support the role of EPS in barite precipitation. The association with barite can correspond to soluble EPS and to cell-bound EPS, which form as a mucilaginous matrix in which cells are also embedded (e.g., Pannard et al., 2016). These cell-bound EPS are a component of the widely studied -Transparent Exopolymer Particles- (TEP) in aquatic ecosystems (Passow and Alldredge, 1995). In general, the attachment of microbes to TEP surfaces and to each other provides higher environmental stability in comparison to free-living (non-attached) cells. Much progress has been made during the last few decades in the understanding of the occurrence of microorganisms in biofilm state in the ocean water column and its impact on ocean processes (e.g., Decho and Gutierrez, 2017). Nonetheless, the role of exopolymers in barite precipitation in the ocean was not explored. More is known about the role of EPS in carbonate precipitation since bacterial mats are well-known for their association with the biogeochemical precipitation of calcite and aragonite (e.g. Braissant et al., 2003, 2007, 2009). It has also been demonstrated that living cells are not always required for microbially mediated carbonates formation, but carbonates can precipitate in the

EPS without the presence of bacteria (Bontognali et al., 2014). This opens an exciting field of research to investigate the potential role of TEP in the ocean water column as substances for bioaccumulation of metals in general and specifically for barite nucleation and growth. TEP occurs in the water column suspended in colloidal form, and is probably formed by the aggregation of smaller EPS molecules (Engel et al., 2004). The abundance of TEP drastically increases during periods of phytoplankton blooms, which further supports the link between export production and barite formation in seawater.

## 5. Conclusions

Observations from suspended marine particulate matter from the North Atlantic and the Southern Ocean show the formation of barite through an initial amorphous phase, rich in P, to which Ba binds and ripens to barite crystals once the phosphate groups are substituted by sulfate. Mineralogical and crystallographic features of these precipitates have provided new insights into this formation process: i) the evolution from Ba-phosphate to Ba-sulfate (i.e., barite) is evidenced by the compositional range identified; ii) the Ba-phosphate precursor is amorphous, and it evolves to crystalline barite; iii) barite itself in association with EPS and organic rich aggregates, which further support the role of

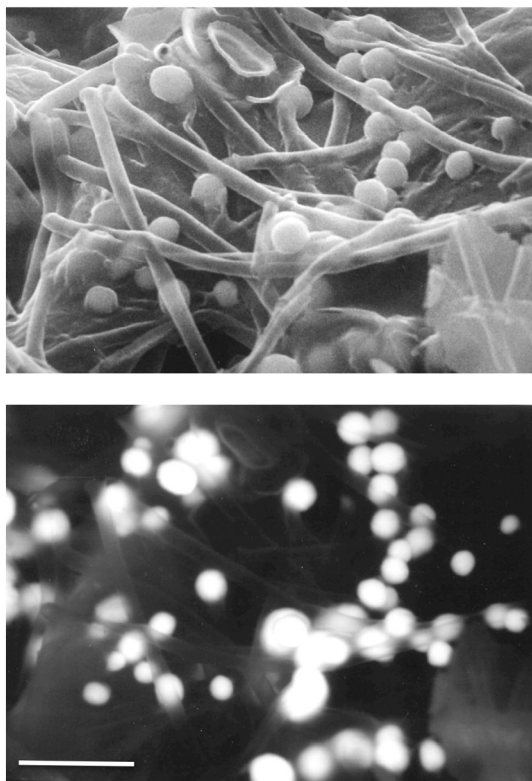


Fig. 9. SEM photographs showing possibly barite mineralized coccus bacteria with typical round morphologies obtained in secondary electron (upper) and backscattered electron mode (lower). Scale bar is 4  $\mu\text{m}$ .

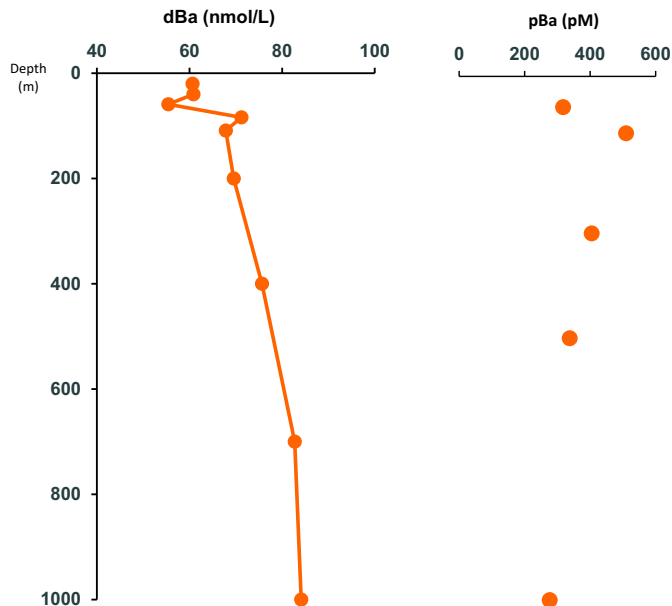


Fig. 10. Dissolved Ba (dBa) and particulate Ba (pBa) concentration (1–51  $\mu\text{m}$  size fraction) profiles at station 92 in the Southern Ocean.

biofilms as Ba-concentrating agents. These micro-scale processes support observed empirical linkages between organic matter degradation, bacterial production, and barite formation. Hence, several lines of evidence support that barite formation mechanisms include Ba bioaccumulation on microbial biofilms, and particularly in EPS, offering a link between bacterial activity and marine barite formation and accumulation in the open ocean.

## Acknowledgments

This study was supported by the European Regional Development Fund (ERDF) co-financed grants CGL2015-66830-R and CGL2017-92600-EXP (MINECO Secretaría de Estado de Investigación, Desarrollo e Innovación, Spain), Research Group RNM-179 and BIO 103 (Consejería de Economía, Innovación, Ciencia y Empleo, Junta de Andalucía) and the University of Granada (Unidad Científica de Excelencia UCE-PP2016-05). We thank the Center for Scientific Instrumentation (CIC, University of Granada), the Warm Core Rings project, and NSF OCE-0961660 for supporting sample collection during MV1101. We also thank editors and two anonymous reviewers for helpful comments that have significantly improved this contribution.

## References

- Balch, W.M., Bates, N.R., Lam, P.J., Twining, B.S., Rosengard, S.Z., Bowler, B.C., Drapeau, D.T., Garley, R., Lubelczyk, L.C., Mitchell, C., Rauschenberg, S., 2016. Factors regulating the Great Calcite Belt in the Southern Ocean and its biogeochemical significance. *Glob. Biogeochem. Cycles* 30, 1124–1144. <https://doi.org/10.1002/2016GB005414>.
- Bates, S.L., Hendry, K.R., Pryer, H.V., Kinsley, C.W., Pyle, K.M., Woodward, E.M.S., Horner, T.J., 2017. Barium isotopes reveal role of ocean circulation on barium cycling in the Atlantic. *Geochim. Cosmochim. Acta* 204, 286–299. <https://doi.org/10.1016/j.gca.2017.01.043>.
- Bertram, M.A., Cowen, J.P., 1997. Morphological and compositional evidence for biotic precipitation of marine barite. *J. Mar. Res.* 55, 577–593. <https://doi.org/10.1357/0022240973224292>.
- Bishop, J.K.B., 1988. The barite-opal-organic carbon association in oceanic particulate matter. *Nature* 332, 341–343.
- Bishop, J.K.B., Wood, T.J., 2008. Particulate matter chemistry and dynamics in the twilight zone at VERTIGO ALOHA and K2 sites. *Deep-Sea Res. I Oceanogr. Res. Pap.* 55, 1684–1706. <https://doi.org/10.1016/j.dsr.2008.07.012>.
- Bishop, J.K.B., Schupack, D., Sherrell, R.M., Conte, M., 1985. A multiple-unit large-volume in situ filtration system for sampling oceanic particulate matter in mesoscale environments. In: *Mapping Strategies in Chemical Oceanography, Advances in Chemistry*. American Chemical Society, pp. 155–175–9. <https://doi.org/10.1021/ba-1985-0209.ch009>.
- Bishop, J.K.B., Lam, P.J., Wood, T.J., 2012. Getting good particles: accurate sampling of particles by large volume in-situ filtration. *Limnol. Oceanogr. Methods* 10, 681–710. <https://doi.org/10.4319/lom.2012.10.681>.
- Bonny, S.M., Jones, B., 2008. Experimental precipitation of barite (BaSO<sub>4</sub>) among streamers of sulfur-oxidizing bacteria. *J. Sediment. Res.* 78, 357–365.
- Bontognali, T.R.R., McKenzie, J.A., Warthmann, R.J., Vasconcelos, C., 2014. Microbially influenced formation of Mg-calcite and Ca-dolomite in the presence of exopolymeric substances produced by sulphate-reducing bacteria. *Terra Nova* 26, 72–77. <https://doi.org/10.1111/ter.12072>.
- Braissant, O., Cailleau, G., Dupraz, C., Verrecchia, E., 2003. Bacterially induced mineralization of calcium carbonate in terrestrial environments: the role of exopolysaccharides and amino acids. *J. Sediment. Res.* 73, 485–490. <https://doi.org/10.1306/111302730485>.
- Braissant, O., Decho, A.W., Dupraz, C., Glunk, C., Przekop, K.M., Visscher, P.T., 2007. Exopolymeric substances of sulfate-reducing bacteria: Interactions with calcium at alkaline pH and implication for formation of carbonate minerals. *Geobiology* 5, 401–411. <https://doi.org/10.1111/j.1472-4669.2007.00117.x>.
- Braissant, O., Decho, A.W., Przekop, K.M., Gallagher, K.L., Glunk, C., Dupraz, C., et al., 2009. Characteristics and turnover of exopolymeric substances in a hypersaline microbial mat. *FEMS Microbiol. Ecol.* 67, 293–307. <https://doi.org/10.1111/j.1574-6941.2008.00614.x>.
- Bridgestock, L., Te Hsieh, Y., Porcelli, D., Homoky, W.B., Bryan, A., Henderson, G.M., 2018. Controls on the barium isotope compositions of marine sediments. *Earth Planet. Sci. Lett.* 481, 101–110. <https://doi.org/10.1016/j.epsl.2017.10.019>.
- Cao, Z., Siebert, C., Hathorne, E.C., Dai, M., Frank, M., 2016. Constraining the oceanic barium cycle with stable barium isotopes. *Earth Planet. Sci. Lett.* 434, 1–9. <https://doi.org/10.1016/j.epsl.2015.11.017>.
- Chow, T.J., Goldberg, E.D., 1960. On the marine geochemistry of barium. *Geochim. Cosmochim. Acta* 20, 192–198. [https://doi.org/10.1016/0016-7037\(60\)90073-95](https://doi.org/10.1016/0016-7037(60)90073-95).
- Decho, A.W., Gutierrez, T., 2017. Microbial extracellular polymeric substances (EPSs) in Ocean systems. *Front. Microbiol.* 8, 922. <https://doi.org/10.3389/fmicb.2017.00922>.
- Dehairs, F., Cheslelet, R., Jedwab, J., 1980. Discrete suspended particles of barite and the barium cycle in the open ocean. *Earth Planet. Sci. Lett.* 49, 528–550. [https://doi.org/10.1016/0012-821X\(80\)90094-1](https://doi.org/10.1016/0012-821X(80)90094-1).
- Dehairs, F., Stroobants, N., Goeyens, L., 1991. Suspended barite as a tracer of biological activity in the Southern Ocean. *Mar. Chem.* 35, 399–410. [https://doi.org/10.1016/S0304-4203\(09\)90032-9](https://doi.org/10.1016/S0304-4203(09)90032-9).
- Dehairs, F., Shopova, D., Ober, S., Veth, C., Goeyens, L., 1997. Particulate barium stocks and oxygen consumption in the Southern Ocean mesopelagic water column during spring and early summer: relationship with export production. *Deep-Sea Res. II Top. Stud. Oceanogr.* 44, 497–516. [https://doi.org/10.1016/S0967-0645\(96\)00072-0](https://doi.org/10.1016/S0967-0645(96)00072-0).
- Dehairs, F., Jacquet, S., Savoye, N., Van Mooy, B.A.S., Buesseler, K.O., Bishop, J.K.B.,

- Lamborg, C.H., Elskens, M., Baeyens, W., Boyd, P.W., Casciotti, K.L., Monnin, C., 2008. Barium in twilight zone suspended matter as a potential proxy for particulate organic carbon remineralization: results for the North Pacific. *Deep-Sea Res. II Top. Stud. Oceanogr.* 55, 1673–1683. <https://doi.org/10.1016/j.dsr2.2008.04.020>.
- Dymond, J., Suess, E., Lyle, M., 1992. Abstract. We used sediment traps to define the higher barium contents in the intermediate and combined our particle flux data with existing water linkages to ocean productivity and the degree of. *Paleoceanography* 7, 163–181.
- Engel, A., Delille, B., Jacquet, S., Riebesell, U., Rochelle-Newall, E., Terbruggen, A., et al., 2004. Transparent exopolymer particles and dissolved organic carbon production by *Emiliania huxleyi* exposed to different CO<sub>2</sub> concentrations: a mesocosm experiment. *Aquat. Microb. Ecol.* 34, 93–104. <https://doi.org/10.3354/ame034093>.
- Ganeshram, R.S., François, R., Commeau, J., Brown-Leger, S.L., 2003. An experimental investigation of barite formation in seawater. *Geochim. Cosmochim. Acta* 67, 2599–2605. [https://doi.org/10.1016/S0016-7037\(03\)00164-9](https://doi.org/10.1016/S0016-7037(03)00164-9).
- Gingele, F., Dahmke, A., 1994. Discrete barite particles and barium as tracers of paleo-productivity in South Atlantic sediments. *Paleoceanography* 9, 151–168. <https://doi.org/10.1029/93PA02559>.
- Glamoclija, M., Garrel, L., Berthon, J., López-García, P., 2004. Biosignatures and bacterial diversity in hydrothermal deposits of Solfatar Crater, Italy. *Geomicrobiol. J.* 21, 529–541. <https://doi.org/10.1080/01490450490888235>.
- González-Muñoz, M.T., Fernández-Luque, B., Martínez-Ruiz, F., Chekroun, K. Ben, Arias, J.M., Rodríguez-Gallego, M., Martínez-Cañamero, M., De Linares, C., Paytans, A., 2003. Precipitation of barite by *Myxococcus xanthus*: possible implications for the biogeochemical cycle of barium. *Appl. Environ. Microbiol.* 69, 5722–5725. <https://doi.org/10.1128/AEM.69.9.5722-5725.2003>.
- González-Muñoz, M.T., Martínez-Ruiz, F., Morcillo, F., Martín-Ramos, J.D., Paytan, A., 2012. Precipitation of barite by marine bacteria: a possible mechanism for marine barite formation. *Geology* 40. <https://doi.org/10.1130/G33006.1>.
- Griffith, E.M., Paytan, A., 2012. Barite in the ocean - occurrence, geochemistry and paleoceanographic applications. *Sedimentology* 59, 1817–1835. <https://doi.org/10.1111/j.1365-3091.2012.01327.x>.
- Hanor, J.S., 2000. Barite–Celestine geochemistry and environments of formation. *Rev. Mineral. Geochem.* 40, 193–275. <https://doi.org/10.2138/rmg.2000.40.4>.
- Horner, T.J., Kinsley, C.W., Nielsen, S.G., 2015. Barium-isotopic fractionation in seawater mediated by barite cycling and oceanic circulation. *Earth Planet. Sci. Lett.* 430, 511–522. <https://doi.org/10.1016/j.epsl.2015.07.027>.
- Horner, T.J., Pryer, H.V., Nielsen, S.G., Crockford, P.W., Gauglitz, J.M., Wing, B.A., Ricketts, R.D., 2017. Pelagic barite precipitation at micromolar ambient sulfate. *Nat. Commun.* 8, 1–11. <https://doi.org/10.1038/s41467-017-01229-5>.
- Jacquet, S.H.M., Dehairs, F., Rintoul, S., 2004. A high resolution dissolved barium transect in the Southern Ocean. *Geophys. Res. Lett.* 31, L14301. <https://doi.org/10.1029/2004GL020016>.
- Jacquet, S.H.M., Dehairs, F., Dumont, I., Becquevort, S., Cavagna, A.J., Cardinal, D., 2011. Twilight zone organic carbon remineralization in the Polar Front Zone and Subantarctic Zone south of Tasmania. *Deep-Sea Res. II Top. Stud. Oceanogr.* 58, 2222–2234. <https://doi.org/10.1016/j.dsr2.2011.05.029>.
- Keasling, J.D., Hupf, G.A., 1996. Genetic manipulation of polyphosphate metabolism affects cadmium tolerance in *Escherichia coli*. *Appl. Environ. Microbiol.* 62, 743–746.
- Kikuchi, T., Tanaka, S., 2012. Biological removal and recovery of toxic heavy metals in water environment. *Crit. Rev. Environ. Sci. Technol.* 42, 1007–1057. <https://doi.org/10.1016/j.jece.2013.12.019>.
- Kuyucak, N., Volesky, B., 1988. Biosorbents for recovery of metals from industrial solutions. *Biotechnol. Lett.* 10, 137–142. <https://doi.org/10.1007/BF01024641>.
- Martin, J.H., Knauer, G.A., Karl, D.M., Broenkow, W.W., 1987. Vertex – carbon cycling in the Northeast Pacific. *Deep-Sea Res. II Top. Stud. Oceanogr.* 34, 267–285. <https://doi.org/10.1357/002224091784995882>.
- Martínez-Ruiz, F., Jroundi, F., Paytan, A., Guerra-Tschuschke, I., Abad, M.M., González-Muñoz, M.T., 2018. Barium bioaccumulation by bacterial biofilms and implications for Ba cycling and use of Ba proxies. *Nat. Commun.* 9, 1619. <https://doi.org/10.1038/s41467-018-04069-z>.
- Merroun, M.L., 1999. Biosorption of metals by *Myxococcus xanthus*. PhD Thesis. University of Granada, Spain.
- Merroun, M.L., Selenska-Pobell, S., 2008. Bacterial interactions with uranium: an environmental perspective. *J. Contam. Hydrol.* 102, 285–295. <https://doi.org/10.1016/j.jconhyd.2008.09.019>.
- Miot, J., Benzerara, K., Morin, G., Kappler, A., Bernard, S., Obst, M., et al., 2009. Iron biomineralization by anaerobic neutrophilic iron-oxidizing bacteria. *Geochim. Cosmochim. Acta* 73, 696–711. <https://doi.org/10.1016/j.gca.2008.10.033>.
- Monnin, C., Jeandel, C., Cattaldo, T., Dehairs, F., 1999. The marine barite saturation state of the world's oceans. *Mar. Chem.* 65, 253–261. [https://doi.org/10.1016/S0304-4203\(99\)00016-X](https://doi.org/10.1016/S0304-4203(99)00016-X).
- Morcillo, F., González-Muñoz, M.T., Reitz, T., Romero-González, M.E., Arias, J.M., Merroun, M.L., 2014. Biosorption and biomineralization of U(VI) by the marine bacterium *Idiomarina loihiensis* MAH1: effect of background electrolyte and pH. *PLoS One*, e91305. <https://doi.org/10.1371/journal.pone.0091305>.
- Pannard, A., Pédrone, J., Bormans, M., Briand, E., Clauquin, P., Lagadeuc, Y., 2016. Production of exopolymers (EPS) by cyanobacteria: impact on the carbon-to-nutrient ratio of the particulate organic matter. *Aquat. Ecol.* 50, 29–44. <https://doi.org/10.1007/s10452-015-9550-3>.
- Passow, U., Alldredge, A.L., 1995. Aggregation of a diatom bloom in a mesocosm: the role of transparent exopolymer particles (TEP). *Deep-Sea Res. II Top. Stud. Oceanogr.* 42, 99–109. [https://doi.org/10.1016/0967-0645\(95\)00006-C](https://doi.org/10.1016/0967-0645(95)00006-C).
- Paytan, A., Griffith, E.M., 2007. Marine barite: recorder of variations in ocean export productivity. *Deep-Sea Res. II Top. Stud. Oceanogr.* 54, 687–705. <https://doi.org/10.1016/j.dsr2.2007.01.007>.
- Paytan, A., Kastner, M., Chavez, F.P., 1996. Glacial to interglacial fluctuations in productivity in the equatorial Pacific as indicated by marine barite. *Science* 274, 1355–1357. <https://doi.org/10.1126/science.274.5291.1355>.
- Planchon, F., Cavagna, A.J., Cardinal, D., André, L., Dehairs, F., 2013. Late summer particulate organic carbon export and twilight zone remineralisation in the Atlantic sector of the Southern Ocean. *Biogeosciences* 10, 803–820. <https://doi.org/10.5194/bg-10-803-2013>.
- Pyle, K.M., Hendry, K.R., Sherrell, R.M., Legge, O., Hind, A.J., Bakker, D., Venables, H., Meredith, M.P., 2018. Oceanic fronts control the distribution of dissolved barium in the Southern Ocean. *Mar. Chem.* <https://doi.org/10.1016/j.marchem.2018.07.002>. In press.
- Qian, C., Yu, X., Wang, X., 2018. A study on the cementation interface of bio-cement. *Mater. Charact.* 136, 122–127. <https://doi.org/10.1016/j.matchar.2017.12.011>.
- Rinaudo, C., Lanfranco, A.M., Franchini-Angela, M., 1994. The system CaHPO<sub>4</sub>·2H<sub>2</sub>O·CaSO<sub>4</sub>·2H<sub>2</sub>O: crystallizations from calcium phosphate solutions in the presence of SO<sub>2</sub><sup>-4</sup>. *J. Cryst. Growth* 142, 184–192. [https://doi.org/10.1016/0022-0248\(94\)90287-9](https://doi.org/10.1016/0022-0248(94)90287-9).
- Rivadeneira, M.A., Martín-Algarra, A., Sánchez-Román, M., Sánchez-Navas, A., Martín-Ramos, J.D., 2010. Amorphous Ca-phosphate precursors for Ca-carbonate biominerals mediated by *Chromohalobacter marismortui*. *ISME J.* 4, 922–932. <https://doi.org/10.1038/ismej.2010.17>.
- Rosengard, S., Lam, P., Balch, W., Auro, M., Pike, S., Drapeau, D., Bowler, B., 2015. Carbon export and transfer to depth across the Southern Ocean Great Calcite Belt. *Biogeosciences* 12, 3953–3971. <https://doi.org/10.5194/bg-12-3953-2015>.
- Rushdi, A.I., McManus, J., Collier, R.W., 2000. Marine barite and celestine saturation in seawater. *Mar. Chem.* 69, 19–31. [https://doi.org/10.1016/S0304-4203\(99\)00089-4](https://doi.org/10.1016/S0304-4203(99)00089-4).
- Sanchez-Moral, S., Luque, L., Cañaveras, J.C., Laiz, L., Jurado, V., Hermosin, B., Saiz-Jimenez, C., 2004. Bioinduced barium precipitation in *St. Callixtus* and *Domitilla* catacombs. *Ann. Microbiol.* 54, 1–12.
- Sanchez-Navas, A., Martín-Algarra, A., 2001. Genesis of apatite in phosphate stromatolites. *Eur. J. Mineral.* 13, 361–376. <https://doi.org/10.1127/0935-1221/01/0013-0361>.
- Secco, M., Lampronti, G.I., Schlegel, M.C., Maritan, L., Zorzi, F., 2015. Degradation processes of reinforced concretes by combined sulfate-phosphate attack. *Cem. Concr. Res.* 68, 49–63. <https://doi.org/10.1016/j.cemconres.2014.10.023>.
- Senko, J.M., Campbell, B.S., Henriksen, J.R., Elshahed, M.S., Dewers, T.A., Krumholz, L.R., 2004. Barite deposition resulting from phototrophic sulfide-oxidizing bacterial activity. *Geochim. Cosmochim. Acta* 68, 773–780. <https://doi.org/10.1016/j.gca.2003.07.008>.
- Sheshadri, S., Prakash, A., Kowshik, M., 2012. Biosynthesis of silver nanoparticles by marine bacterium, *Idiomarina* sp. PR58-8. *Bull. Mater. Sci.* 35, 1201–1205. <https://doi.org/10.1007/s12034-012-0417-0>.
- Singer, D.M., Griffith, E.M., Senko, J.M., Fitzgibbon, K., Widanagamage, I.H., 2016. Celestine in a sulfidic spring barite deposit—a potential biomarker? *Chem. Geol.* 440, 15–25. <https://doi.org/10.1016/j.chemgeo.2016.05.035>.
- Stevens, E.W.N., Bailey, J.V., Flood, B.E., Jones, D.S., Gilhooly, W.P., Joye, S.B., Teske, A., Mason, O.U., 2015. Barite encrustation of benthic sulfur-oxidizing bacteria at a marine cold seep. *Geobiology* 13, 588–603. <https://doi.org/10.1111/gbi.12154>.
- Stroobants, N., Dehairs, F., Goeyens, L., Vanderheijden, N., Van Grieken, R., 1991. Barite formation in the Southern Ocean water column. *Mar. Chem.* 35, 411–421. [https://doi.org/10.1016/S0304-4203\(99\)90033-0](https://doi.org/10.1016/S0304-4203(99)90033-0).
- Tazaki, K., Webster, J., Fyfe, W.S., 1997. Transformation processes of microbial barite to sediments in Antarctica. *Jpn. J. Geol.* 26, 63–68.
- Torres-Crespo, N., Martínez-Ruiz, F., González-Muñoz, M.T., Bedmar, E.J., De Lange, G.J., Jroundi, F., 2015. Role of bacteria in marine barite precipitation: a case study using Mediterranean seawater. *Sci. Total Environ.* 512, 562–571. <https://doi.org/10.1016/j.scitotenv.2015.01.044>.
- Van Beek, P., Reyss, J.-L., Bonte, P., Schmidt, S., 2003. Sr/Ba in barite: a proxy of barite preservation in marine sediments? *Mar. Geol.* 199, 205–220. [https://doi.org/10.1016/S0025-3227\(03\)00220-2](https://doi.org/10.1016/S0025-3227(03)00220-2).
- Widanagamage, I.H., Griffith, E.M., Singer, D.M., Scher, H.D., Buckley, W.P., Senko, J.M., 2015. Controls on stable Sr-isotope fractionation in continental barite. *Chem. Geol.* 411, 215–227. <https://doi.org/10.1016/j.chemgeo.2015.07.011>.